CrystEngComm

Accepted Manuscript

CrystEngComm

Dynamic Article Links ►

Cite this: DOI: 10.1039/c5ce00000x

www.rsc.org/CrystEngComm

ARTICLE

Assembly of A Series of d^{10} Coordination Polymers Based on W-shaped 1,3-Di(2',4'-dicarboxylphenyl)benzene: From Syntheses, Structural Diversity, Luminescence, to Photocatalytic Properties

Xiutang Zhang,*[a,b] Liming Fan,[a,b] Weiliu Fan,[b] Bin Li[a] and Xian Zhao*[b]

Received (in XXX, XXX) Xth XXXXXXXXX 2015, Accepted Xth XXXXXXXXX 2015
DOI: 10.1039/c5ce00000x

ABSTRACT: Solvothermal reactions of W-shaped 1,3-di((2',4'-dicarboxylphenyl)benzene (H_4DDB) and zinc (II) or cadmium (II) salts in the presence or absence of three ancillary bridging imidazole linkers afford six CPs, namely, $[Zn(H_2DDB)(H_2O)_2(\mu_2\text{-}H_2O)]_n$ (**1**), $[Zn_2(DDB)(1,4\text{-bimb})]_n$ (**2**), $[Zn_2(DDB)(1,3\text{-bimb})]_n$ (**3**), $\{[Zn_4(DDB)(HDDB)(1,3\text{-bmib})_2Cl]\cdot H_2O\}_n$ (**4**), $\{[Cd_2(DDB)(1,3\text{-bimb})]\cdot H_2O\}_n$ (**5**), and $\{[Cd_2(DDB)(1,3\text{-bmib})(H_2O)_{0.5}]\cdot H_2O\}_n$ (**6**), (1,3-bimb = 1,3-bis(imidazol-1-ylmethyl)benzene, 1,4-bimb = 1,4-bis(imidazol-1-ylmethyl)benzene, and 1,3-bmib = 1,3-bis(2-methylimidazol-1-ylmethyl)benzene). Complex **1** is a $[Zn(H_2DDB)(H_2O)_2(\mu_2\text{-}H_2O)]_n$ chain, which are further extended to a 3D supramoelcular structure *via* the hydrogen bonds. Complexes **2** and **3** exhibit the same (3,4,6)-connected net with the Schläfli symbol of $(5^2\cdot6^2\cdot8\cdot9)(5^2\cdot6)_2(5^4\cdot6^4\cdot7^2\cdot8^3\cdot9\cdot10)$ built from two kinds $[Zn_2(COO)_4]$ and $[Zn_2(COO)_2]$ SBUs. While complex **4** is an another (3,4,6)-connected net with the Schläfli symbol of $(3\cdot4\cdot5\cdot6^2\cdot7)(3\cdot4\cdot5\cdot6^7\cdot7^3\cdot8^2)(3\cdot7^2)$, based on the same $[Zn_2(COO)_2]$ and $[Zn_2(COO)_4]$ SBUs. The two Cd^{II} complexes of **5** and **6** display 3D (3,10)-connected $(4^{10}\cdot6^{32}\cdot8^3)(4^3)_2$ nets, consisting of $\{Cd_4(COO)_8\}$ and $[Cd_4(COO)_8(\mu_2\text{-}H_2O)]$ SBUs, respectively. The thermal stability and luminescence properties of complexes **1**-**6** have been investigated. In addition, complexes **1**-**6** show excellent photocatalytic activity for dye methylene orange (MO) degradation in aqueous solution under UV light. And complexes **2**–**6** exhibited relatively good chemical stability in aqueous solutions with pH regulated from 2 to 12.

Introduction

Metal–organic coordination polymers (CPs), as an emerging lass of inorganic–organic hybrid materials, have attracted increasing research interest not only because of their diverse structures and interesting topologies but also owing to their tremendous potential applications in gas storage and separation, magnetism, luminescence, nonlinear optics, drug delivery, photocatalytic, and heterogeneous catalysis.[1–4] Despite the breathtaking achievements in this synthetic aspect, to predict and further accurately control the framework array of a given crystalline product still remain a considerable challenge at this stage.[5,6]

Generally, the structural diversities of the designed CPs are mainly affected by the subtle intrinsic and external parameters (the different coordination preferences of metal ion, templating agents, metal-ligand ratio, pH value, counteranion, and so on).[7-9] Among these factors, the rational selection of organic ligands or coligands according to their length, rigidity and functional groups is important for the assembly of structural controllable CPs, and a great deal of significant works have been done by using this strategy.[10] Among which, the V-shaped polycarxobylates (such as, 4,4′-dicarboxydiphenylamine, 4,4′-oxybis(benzoate) acid, 4-(4-carboxyphenoxy)phthalate acid, 2,2′-azanediyldibenzoic acid, 5-(4-carboxy-2-nitrophenoxy)isophthalic acid, and 4,4′-(hexafluoroisopropylidene)bis(benzoic acid)) with flexible, semirigid or rigid bent backbones have been paid much attention due to their rich coordination modes.[11-13] Whereas, the W-shaped tetracarboxylate linkers are rarely employed in the construction of functional coordination polymers.

Recent study on coordination assemblies by using 2,6-bis(3,5-dicarboxyphenyl)pyridine (H_4BDP) and bis(imidazole) linker states a reliable strategy for obtaining unique nets.[10d] Also, a minor change of the polycarboxylic acids building blocks may be applied to realize good structural control of the resulted metal-organic polymers. Thus, these considerations inspired us to explore new coordination frameworks with W-shaped 1,3-di(2',4'-dicarboxylphenyl)benzene (H_4DDB) ligand and d^{10} metal salts under solvothermal conditions in the presence of three flexible bis(imidazole) linkers (shown in Scheme 1). Their structures ranged from 1D chain based supramolecular structure (**1**), $[Zn_2(COO)_4]$ and $[Zn_2(COO)_2]$ SBUs based Zn(II) CPs with (3,4,6)-connected $(5^2\cdot6^2\cdot8\cdot9)(5^2\cdot6)_2(5^4\cdot6^4\cdot7^2\cdot8^3\cdot9\cdot10)$ net (**2** and **3**), (3,4,6)-connected $(3\cdot4\cdot5\cdot6^2\cdot7)(3\cdot4\cdot5\cdot6^7\cdot7^3\cdot8^2)(3\cdot7^2)$ net (**4**), to

[a] *Advanced Material Institute of Research, College of Chemistry and Chemical Engineering, Qilu Normal University, Jinan, 250013, China. E-mail: xiutangzhang@163.com.*
[b] *State Key Laboratory of Crystal Materials, Shandong University , Jinan 250100, China. E-mail: zhaoxian@sdu.edu.cn.*

†Electronic Supplementary Information (ESI) available: Additional Figures, IR spectrum, TG, PXRD patterns and X-ray crystallographic data CCDC: 1049586 for **1**, 1049587 for **2**, 1049588 for **3**, 1049589 for **4**, 1401535 for **5**, and 1401536 for **6**. See DOI: 10.1039/c5ce00000x.

$[Cd_4(COO)_8]$ or $[Cd_4(COO)_8(\mu_2\text{-}H_2O)]$ SBUs based Cd(II) CPs with (3,10)-connected $(4^{10}\cdot6^{32}\cdot8^3)(4^3)_2$ net (**5** and **6**). All the 3D nets are noninterpenetrated, and their topologies have never been documented up to now. Moreover, complexes **1-6** show relatively good photocatalytic activity for dye methylene orange (MO) degradation in aqueous solution under UV light.

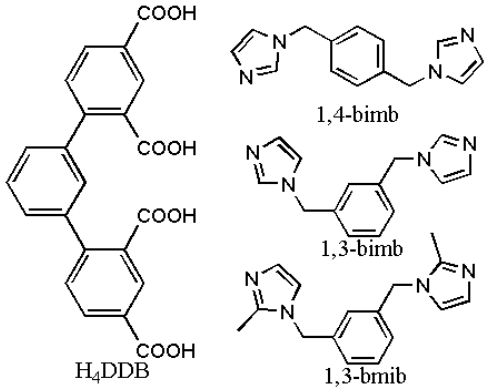

Scheme 1. Structures of H_4DDB and ancillary bridging imidazole linkers.

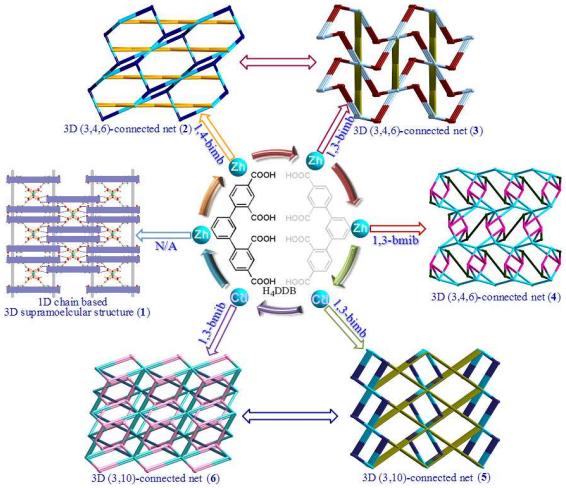

Scheme 2. Diversified polymeric structures of complexes **1–6.**

Experimental Section

Materials and Methods. All the chemical reagents were purchased from Jinan Henghua Sci. & Tec. Co. Ltd. without further purification. IR spectra were measured on a NEXUS 670 FTIR spectrometer. Elemental analyses were carried out on a CE instruments EA 1110 elemental analyzer. Thermogravimetric analyses (TGA) were performed under air condition on Perkin-Elmer TGA-7 thermogravimetric analyzer. X-ray powder diffractions were measured on a Panalytical X-Pert pro diffractometer with Cu-Kα radiation. Fluorescence spectra were performed on a Hitachi F-4500 fluorescence spectrophotometer at room temperature. Photocatalytic experiments in aqueous solutions were performed in a 30 mL test tube. A 125 W high-pressure mercury lamp was used as the UV light source. 0.5 mL 30% hydrogen peroxide was injected into 30 min dark adsorption pretreated 20.0 mL 2.5×10^{-5} mol L^{-1} methylene orange (MO) aqueous solution with 5 mg of powdered catalyst. At given irradiation time intervals, a series of aqueous solutions of a certain volume were collected and separated through a centrifuge to remove suspended catalyst particles and then subjected to UV−vis spectroscopic measurement. The decomposition of dye methylene orange (MO) was monitored by the characteristic absorption band at 464 nm.

General Synthesis and Characterization. All the titled compelxes are synthesised under simialr conditions with the mixture of H_4DDB, ancillary imidazole linkers, and Zn^{II} or Cd^{II} salts added in H_2O or CH_3CN-H_2O mixed sovlents. The NaOH was added to eliminate the protons of H_4DDB. After 130 °C heated for 5 days, the suitalbe crystals were obtained. For **1-6**, the IR absorption bands in the range of 3400-3500 cm^{-1} can be attributed to the characteristic peaks of O-H vibrations. The vibrations at ca. 1530 and 1620 cm^{-1} correspond to the asymmetric and symmetric stretching vibrations of the carboxyl groups, respectively (Fig. S1).[14]

Complexes **1-6** are insoluble in water and common organic solvents including methanol, ethanol, toluene, and acetonitrile. In order to inversitgte the chemical stability of complexes **1–6**, the crystal samples were soaked into the aqueous solutions with pH values ranging from 2 to 12 (prepared with HCl and NaOH solution respectively) for 24 h, and the PXRD patterns of soaked complexes **2-6** showed no alteration, showed in Fig. S2.

Synthesis of $[Zn(H_2DDB)(H_2O)_2(\mu_2\text{-}H_2O)]_n$ (1). A mixture of H_4DDB (0.13 mmol, 0.051 g), $ZnSO_4\cdot7H_2O$ (0.40 mmol, 0.115 g), NaOH (0.30 mmol, 0.012 g) and 10 mL H_2O was placed in a 25 mL Teflon-lined stainless steel vessel, heated to 130 °C for 3 days, followed by slow cooling (a descent rate of 10 °C/h) to room temperature. Colorless block crystals of **1** were obtained. Yield of 62% (based on H_4DDB). Anal. (%) calcd. for $C_{21}H_{17}NO_{11}Zn$: C, 48.06; H, 3.27; N, 2.67. Found: C, 48.23; H, 3.41; N, 2.70. IR (KBr pellet, cm^{-1}): 3186 (s), 2164 (m), 1689 (vs), 1607 (m), 1562 (m), 1546 (s), 1439 (m), 1421 (s), 1366 (vs), 1215 (s), 1163 (m), 1123 (s), 896 (w), 766 (m), 647 (w).

Synthesis of $[Zn_2(DDB)(1,4\text{-bimb})]_n$ (2). A mixture of H_4DDB (0.10 mmol, 0.041 g), 1,4-bimb (0.30 mmol, 0.071 g), $ZnSO_4\cdot7H_2O$ (0.20 mmol, 0.057 g) was put into the mixed solvent of 6 mL H_2O and 3 mL acetonitrile and then tranformed to a 25 mL Teflon-lined stainless steel vessel, heated to 130 °C for 3 days, followed by slow cooling (a descent rate of 10 °C/h) to room temperature. Colourless block crystals of **2** were obtained. Yield of 75% (based on H_4DDB). Anal. (%) calcd. for $C_{36}H_{24}N_4O_8Zn_2$: C, 56.05; H, 3.14; N, 7.26. Found: C, 55.97; H, 3.19; N, 7.47. IR (KBr pellet, cm^{-1}): 3124 (m), 2972 (m), 1636 (s), 1609 (s), 1577 (m), 1531 (s), 1520 (m), 1448 (m), 1391 (s), 1239 (m), 1116 (m), 1039 (w), 954 (w), 827 (w), 782 (m), 743 (m), 653 (m).

Synthesis of $[Zn_2(DDB)(1,3\text{-bimb})]_n$ (3). The synthetic method is similar to that of compound **2** except that 1,4-bimb was replaced by 1,4-bimb. Colorless block crystals of **3** were obtained. Yield of 37% (based on H_4DDB). Anal. (%) calcd. for $C_{36}H_{24}N_4O_8Zn_2$: C, 56.05; H, 3.14; N, 7.26. Found: C, 56.13; H, 3.17; N, 7.19. IR (KBr pellet, cm^{-1}): 3132 (m), 3029 (w), 2287 (w), 2165 (w), 1723 (m), 1639 (vs), 1610 (s), 1530 (s), 1446 (s), 1390 (vs), 1239 (m), 1116 (s), 1091 (m), 1030 (w), 954 (m), 908 (w), 828 (w), 793 (m), 785 (m), 743 (m), 726 (m), 653 (m).

Table 1 Crystal data for **1 – 6**.

Complex	**1**	**2**	**3**	**4**	**5**	**6**
Empirical formula	$C_{21}H_{17}NO_{11}Zn$	$C_{36}H_{24}N_4O_8Zn_2$	$C_{36}H_{24}N_4O_8Zn_2$	$C_{76}H_{59}ClN_8O_{17}Zn_4$	$C_{36}H_{26}Cd_2N_4O_9$	$C_{76}H_{62}Cd_4N_8O_{19}$
Formula weight	524.73	771.33	771.33	1653.24	883.41	1840.94
Crystal system	Orthorhombic	Monoclinic	Monoclinic	Monoclinic	Monoclinic	Monoclinic
Space group	*Pnma*	$P2_1/n$	$P2_1/n$	$P2_1/n$	$P2_1/c$	$P2_1/c$
a (Å)	7.7017(3)	15.1215(13)	15.3901(12)	21.3597(15)	11.0644(5)	11.1209(5)
b (Å)	22.7746(7)	10.2017(9)	9.9023(8)	10.7751(7)	28.5964(13)	28.4090(14)
c (Å)	11.5195(4)	22.1609(19)	21.9596(17)	31.118(2)	10.4332(5)	10.7889(5)
β (°)	90	107.2813(18)	105.911(3)	92.635(2)	96.5018(15)	96.9478(14)
V(Å^3)	2020.56(12)	3264.3(5)	3218.4(4)	7154.2(8)	3279.9(3)	3383.5(3)
Z	4	4	4	4	4	2
D_{calcd} (Mg/m^3)	1.725	1.569	1.592	1.535	1.789	1.807
μ(mm^{-1})	1.285	1.530	1.552	1.439	1.361	1.324
θ range (°)	3.18–25.00	2.91–25.00	2.90–25.00	2.92–25.00	2.90–25.00	3.15–25.00
Reflections collected	25470	41306	41862	93611	37201	42688
Data/Parameters	1831/171	5728/451	5662/451	12575/968	5751/467	5791/495
F(000)	1072	1568	1568	3376	1752	1836
R_{int}	0.0700	0.0976	0.1230	0.1060	0.0880	0.0666
R_1 (wR_2) [$I > 2\sigma(I)$]^{a,b}	0.0331 (0.0810)	0.0541 (0.1262)	0.0482 (0.0963)	0.0523 (0.1253)	0.1652 (0.4259)	0.0740 (0.1849)
R_1 (wR_2) (all data)^{a,b}	0.0434 (0.0862)	0.0870 (0.1423)	0.1057 (0.1215)	0.0969 (0.1534)	0.2162 (0.4853)	0.0897 (0.1966)
Gof	1.000	1.002	1.005	0.998	1.000	1.003

$^a R_1 = \Sigma| |F_o|-|F_c| | / \Sigma|F_o|$, $^b wR_2 = [\Sigma w(F_o^2-F_c^2)^2]/ \Sigma w(F_o^2)^2]^{1/2}$

Synthesis of {[Zn$_4$(DDB)(HDDB)(1,3-bmib)$_2$Cl]·H$_2$O}$_n$ (4). A mixture of H$_4$DDB (0.10 mmol, 0.041 g), 1,3-bmib (0.30 mmol, 0.077 g), ZnCl$_2$·H$_2$O (0.20 mmol, 0.027 g) was put into the mixed solvent of 6 mL H$_2$O and 3 mL acetonitrile and then tranformed to a 25 mL Teflon-lined stainless steel vessel, heated to 130 °C for 3 days, followed by slow cooling (a descent rate of 10 °C/h) to room temperature. Colourless block crystals of **4** were obtained. Yield of 57% (based on H$_4$DDB). Anal. (%) calcd. for C$_{76}$H$_{59}$ClN$_8$O$_{17}$Zn$_4$: C, 55.21; H, 3.60; N, 6.78. Found: C, 55.13; H, 3.69; N, 6.73. IR (KBr pellet, cm^{-1}): 3125 (m), 3040 (m), 1704 (s), 1643 (vs), 1545 (s), 1506 (m), 1451 (s), 1396 (vs), 1286 (m), 1278 (m), 1248 (w), 1159 (m), 805 (m), 782 (s), 743 (s), 690 (s), 623 (vs).

Synthesis of {[Cd$_2$(DDB)(1,3-bimb)]·H$_2$O}$_n$ (5). The synthetic method is similar to **3** except that ZnSO$_4$·7H$_2$O was replaced by CdSO$_4$. Colorless block crystals of **5** were obtained. Yield of 46% (based on H$_4$DDB). Anal. (%) calcd. for C$_{36}$H$_{26}$Cd$_2$N$_4$O$_9$: C, 48.94; H, 2.97; N, 6.34. Found: C, 48.29; H, 3.03; N, 6.31. IR (KBr pellet, cm^{-1}): 3123 (m), 1572 (vs), 1546 (s), 1518 (s), 1436 (m), 1383 (s), 1294 (m), 1240 (m), 1089 (m), 671 (m), 657 (m).

Synthesis of {[Cd$_2$(DDB)(1,3-bmib)(H$_2$O)$_{0.5}$]·H$_2$O}$_n$ (6). The synthetic method is similar to **5** except that 1,3-bimb was replaced by 1,3-bmib. Colorless block crystals of **6** were obtained. Yield of 52% (based on H$_4$DDB). Anal. (%) calcd. for C$_{76}$H$_{62}$Cd$_4$N$_8$O$_{19}$: C, 49.58; H, 3.39; N, 6.09. Found: C, 49.67; H, 3.41; N, 6.13. IR (KBr pellet, cm^{-1}): 3181 (m), 1573 (vs), 1540 (s), 1508 (s), 1368 (vs), 1376 (m), 1284 (s), 1137 (s), 1049 (m), 740 (s), 6671 (m), 628 (s).

X-ray Crystallography. The crystal data was collected with a Siemens SMART diffractometer using Mo-Kα radiation (λ=0.71073Å) at 296(2) K. The structures of those titled complexes were solved by direct methods, with the non-hydrogen atoms refined anisotropially by using the SHELXTL package with F^2 values based full-matrix least-squares procedure.[15] All the hydrogen atoms except those for water molecules were generated geometrically with fixed isotropic thermal parameters, and included in the structure factor calculations. And the hydrogen atoms attached to oxygen were refined with O–H=0.85Å and U$_{iso}$(H) =1.2U$_{eq}$(O). For **1**–**6**, crystallographic data and the selected bond lengths and angles are given in Table 1 and Table S1. CCDC reference numbers: 1049586 for **1**, 1049587 for **2**, 1049588 for **3**, 1049589 for **4**, 1401535 for **5**, and 1401536 for **6**. Topological analysis was performed by using TOPOS program.[16]

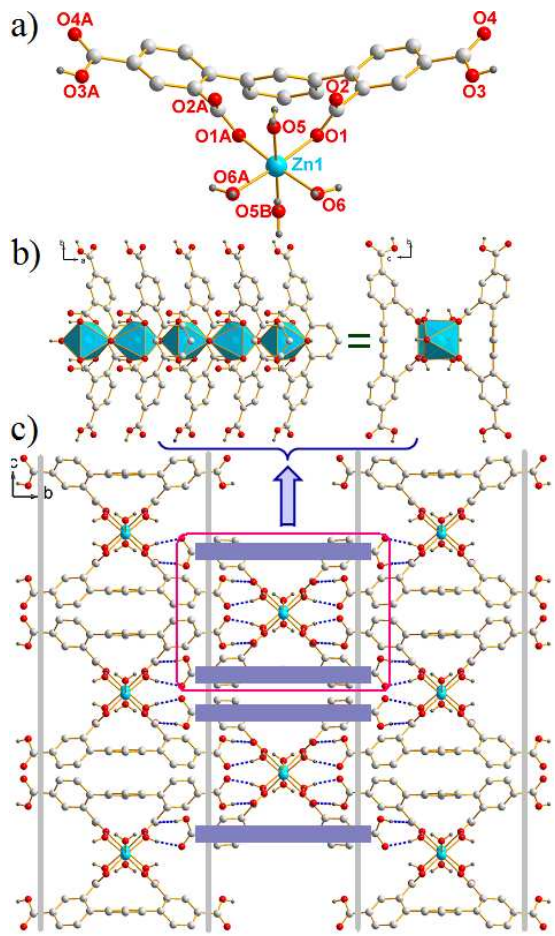

Figure 1. (a) The asymmetric unit of **1** (Symmetry code: A: x, 3/2-y, 1/2-z.). (b) The 1D chain view along c and a directions. (c) View of the 3D supramolecular structure of **1**.

Result and Discussion

Structural Description of $[Zn(H_2DDB)(H_2O)_2(\mu_2\text{-}H_2O)]_n$ (1). Single-crystal determination reveals complex **1** possessed a three-dimension supramolecular structure, built from 1D $[Zn(H_2O)_2(\mu_2\text{-}H_2O)]_n$ chains with the help of O–H···O hydrogen bonds. Complex **1** crystallizes in the orthorhombic system, space group *Pnma*. The asymmetric unit consists of half of Zn^{II} ions, half of H_2DDB^{2-} ligands, one and a half water molecules. In the building unit of **1**, each Zn^{II} ion adopts a distorted octahedral geometry by coordinating to four water molecules and two oxygen atoms of two monodentate carboxyl groups from one H_2DDB^{2-}ligand (Fig. 1a). In **1**, H_2DDB^{2-} is partly deprotonated and adopts the coordination mode of I (Scheme 3). The two dihedral angles between the central phenyl ring and the two side phenyl rings are equal (49.3(4)°). And the dihedral angle between two side phenyl rings is 31.9(1)°. Two 2-position carboxyl groups were deprotonated and coordinated to one Zn^{II} ion. Furthermore, Zn^{II} ions are bridged by μ_2-coordinated water molecules to form 1D $[Ni(H_2O)_2(\mu_2\text{-}H_2O)]_n$ chain (Fig. S3) with the nearest Zn···Zn distance being 3.862 Å (Fig. 1b). Moreover, the neighbouring chains are interacted with each other through O–H···O hydrogen bonds (Table 2) to generate a 3 D supramolecular structure (Fig. 1c).

Table 2 The hydrogen bonds in complex **1**.

Donor–H···Acceptor	d(D–A) (Å)	d(D···H) (Å)	d(H···A) (Å)	∠DHA (º)
O(5)–H(1w)···O(2)	2.626	0.820	2.272	106.74
O(3)--H(3)····O(2)$^{\#1}$	2.740	0.820	1.966	157.27
O(6)--H(4w)····O(4)$^{\#2}$	2.686	0.820	1.880	167.34
O(6)--H(3w)····O(1)$^{\#3}$	2.681	0.820	1.881	167.74
C(8)--H(8)····O(3)$^{\#1}$	3.199	0.930	2.470	157.27

Symmetry codes: #1 -*x*+2, -*y*+1, -*z*+1; #2 -*x*+3/2, -*y*+1, *z*+1/2; #3 *x*+1/2, *y*, -*z*+3/2.

Structural Description of $[Zn_2(DDB)(1,4\text{-bimb})]_n$ (2). The crystal structure analysis reveals that complex **2** crystallized in monoclinic system with the space group of $P2_1/n$. The asymmetric unit consists of two Zn^{II} ions, one completely deprotonated DDB^{4-} ligand, and one 1,4-bimb ligand. As shown in Fig. 2a, the Zn(1) is penta-coordinated by one N atom from 1,4-bimb ligand, and four O atoms from two different DDB^{4-} ligands, leaving a square pyramid coordination geometry with slightly distorted. While Zn(2) is located in a distorted tetrahedron environment, completed by one N atom from 1,4-bimb ligand and three O atoms from two different DDB^{4-} ligands. The Zn−N distances are 1.984(4) Å and 1.992(5) Å, and the Zn−O lengths span in the range of 1.963(3)–2.077(3) Å.

In complex **2**, each DDB^{4-} ligand is completely deprotonated and coordinates with five Zn^{II} ions by using three bridging μ_2-η^1:η^1 carboxyl groups and one monodentate μ_1-η^1:η^0 carboxyl group (Mode II). It is worthy to note that two Zn ions are bridged by the four 2-position carboxyl groups of two DDB^{4-} ligands to form a common $[Zn_2(COO)_4]$ paddle wheel unit, and the $[Zn_2(COO)_2]$ paddle wheel unit for 4-position carboxyl groups (Fig. 2b). Because the nature of DDB^{4-} linkers, they bridging the resulting SBUs into a complicated 3D network with very open channels (Fig. S4). And the 1,4-bimb linkers further fulfil the channels, finally resulting in a 3D network (Fig. 2c).

Topology analysis shows the whole network of complex **2** can be rationalized to an unprecedented 3D trinodal (3,4,6)-connected net with the Point Schläfli Symbol of $(5^2\cdot6^2\cdot8\cdot9)(5^2\cdot6)_2(5^4\cdot6^4\cdot7^2\cdot8^3\cdot9\cdot10)$ by denoting the DDB^{4-} ligand as 3-connected nodes, the $[Zn_2(COO)_4]$ SBUs as 4-connected nodes, and the $[Zn_2(COO)_2]$ SBUs as 6-connected nodes, respectively (Fig. 2d).

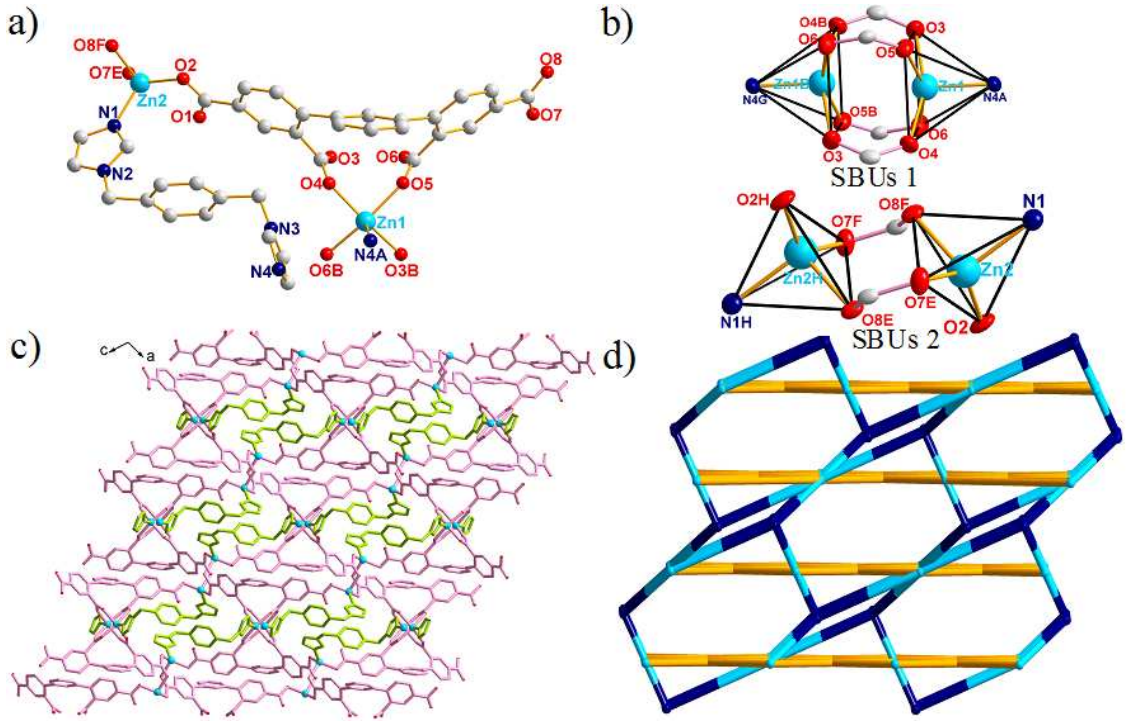

Figure 2. (a) The asymmetric unit of **2** (Symmetry codes: A: 2-*x*, 1-*y*, 2-*z*; B: 2-*x*, 2-*y*, 2-*z*; C: 2-*x*, 2-*y*, 1-*z*; E: 1/2+*x*, 5/2-*y*, -1/2+*z*; F: 3/2-*x*, -1/2+*y*, 3/2-*z*.). (b) Two types of paddlewheel secondary building units (SBUs): $[Zn_2(COO)_2]$ and $[Zn_2(COO)_4]$. (c) Schematic view of the 3D frameworks of complex **2** view along *b* direction. (d) View of the 3D (3,4,6)-connected $(5^2\cdot6^2\cdot8\cdot9)(5^2\cdot6)_2(5^4\cdot6^4\cdot7^2\cdot8^3\cdot9\cdot10)$ topology of **2**.

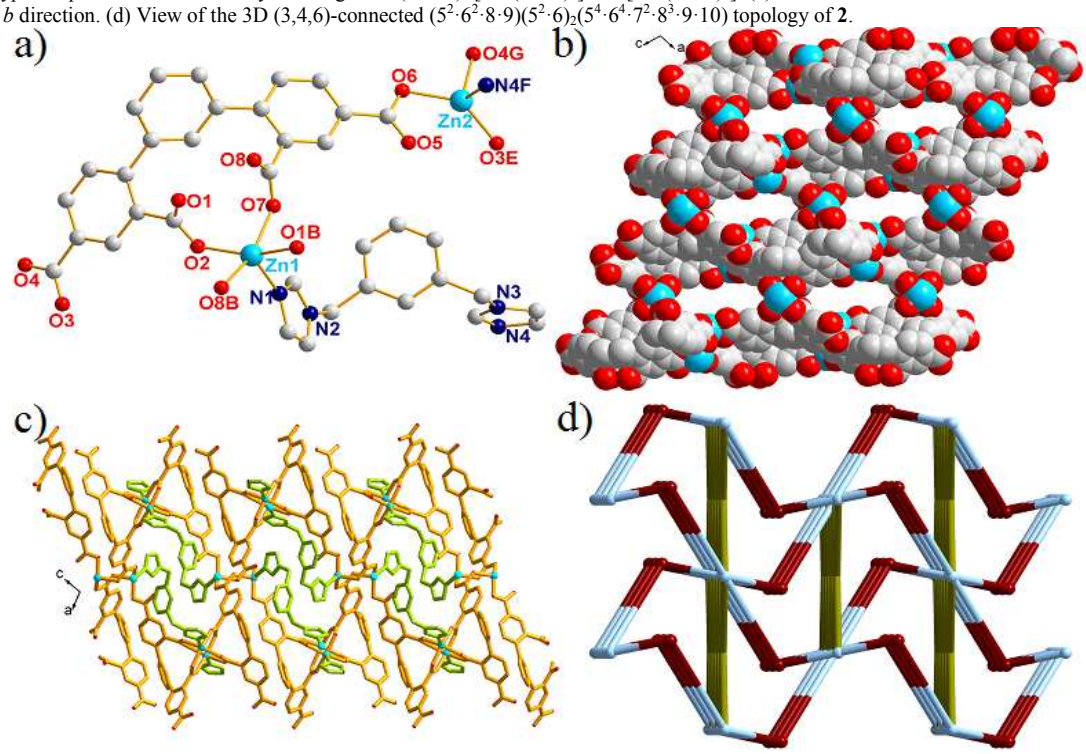

Figure 3. (a) The asymmetric unit of **3** (Symmetry codes: B: 1-*x*, 1-*y*, -*z*; E: -1/2+*x*, 1/2-*y*, 1/2+*z*; F: *x*, 1+*y*, *z*; G: 3/2-*x*, 1/2+*y*, 1/2-*z*.). (b) The 3D $[Zn_2(DDB)]_n$ net view along *b* axis. (c) The 3D networks of complex **3** view along *b* axis. (d) The 3D (3,4,6)-connected $(5^2\cdot6^2\cdot8\cdot9)(5^2\cdot6)_2(5^4\cdot6^4\cdot7^2\cdot8^3\cdot9\cdot10)$ topology of **3**.

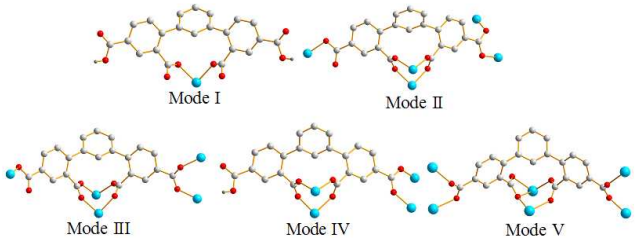

Scheme 3. The coordination modes of H_4DBB in complexes **1**–**6**.

Structural Description of $[Zn_2(DDB)(1,3\text{-bimb})]_n$ (3). When the *para*- 1,4-bimb was replaced by *meta*- 1,3-bimb, a similar 3D zinc CPs with two types of paddlewheel secondary building units (SBUs): $[Zn_2(COO)_4]$, and $[Zn_2(COO)_2]$ have been obtained. Complex **3** crystallizes in monoclinic space group $P2_1/n$. The asymmetric unit contains two crystallographically independent Zn^{II} ions, one 1,3-bimb ligand, and one DDB^{4-} ligand (Fig. 3a). Each Zn(1) is located in a distorted $\{ZnO_4N\}$ square pyramid coordination environment, completed by one N atom from 1,3-bimb ligand and four O atoms from two different DDB^{4-} ligands. And Zn(2) is penta-coordinated by one N atom from 1,3-bimb ligand, and three O atoms from two DDB^{4-} ligands, leaving a tetrahedron coordination geometry with slightly distorted. The Zn−N/O distances are ranged from 1.972(3) to 2.082(3) Å.

Each DDB^{4-} links with two $[Zn_2(COO)_2]$ SBUs and one $[Zn_2(COO)_4]$ SBUs, giving a complicated 3D framework with oval open channels (9.495×14.984 $Å^2$) along *b* direction (Fig. 3b). And then the 1,3-bimb further bridged the adjacent $[Zn_2(COO)_2]$ SBUs and $[Zn_2(COO)_4]$ SBUs, constructing a complicated 3D framework (Fig. 3c). Similar to complex **2**, from the viewpoint of topology, complex **3** is also a (3,4,6)-connected net with $(5^2\cdot6^2\cdot8\cdot9)(5^2\cdot6)_2(5^4\cdot6^4\cdot7^2\cdot8^3\cdot9\cdot10)$ topology (Fig. 3d).

Structure descriptions of $\{[Zn_4(DDB)(HDDB)(1,3\text{-bmib})_2Cl]\cdot H_2O\}_n$ (4). Structural analysis reveals that complex **4** crystallizes in the monoclinic crystal system $P2_1/n$, and the asymmetric unit contains four crystallographically independent Zn^{II} ions, one completely deprotonated DDB^{4-} ligand, one partly deprotonated $HDDB^{3-}$ ligand, one 1,3-bmib ligand, one Cl^-, and one lattice water molecule. Zn (1) and Zn (2) show similar coordination environments, both surrounded by four O atoms from the 2-position carboxyl groups and one N atom from 1,3-bmib. Zn (3) is coordinated by two O atoms from one DDB^{4-} ligand and one $HDDB^{3-}$ ligand, one Cl^-, and one N atom from 1,3-bmib. Zn(4) is four-coordinated, completed by three O atoms from two different DDB^{4-} ligands and one $HDDB^{3-}$ anion, and one N atom from the 1,3-bmib ligand, leaving a distorted tetrahedral coordination geometry. Besides, those Zn^{II} ions attached bond lengths and bond angles around Zn^{II} ions are all span in the normal range.

The DDB^{4-} ligand shows $(\kappa^1\text{-}\kappa^0)\text{-}(\kappa^1\text{-}\kappa^1)\text{-}(\kappa^1\text{-}\kappa^1)\text{-}(\kappa^1\text{-}\kappa^1)\text{-}\mu_5$ (Mode III) linking two $[Zn_2(COO)_2]$ SBUs and one $[Zn_2(COO)_4]$ SBUs, and the $HDDB^{3-}$ ligand displays $(\kappa^1\text{-}\kappa^1)\text{-}(\kappa^1\text{-}\kappa^1)\text{-}(\kappa^1\text{-}\kappa^1)\text{-}\mu_4$ (Mode IV) bridging one $[Zn_2(COO)_2]$ SBUs and one $[Zn_2(COO)_4]$ SBUs, finally given a 2D $[Zn_2(DDB)(HDDB)]_n$ sheet (Fig. 4b). Then those 2D sheets are further expanded to a 3D network by using the 1,3-bmib as pillars (Fig. 4c). And the 1,3-bmib separated Zn···Zn distances are 7.997(8) Å (Zn1-Zn4) and 8.920(0) Å (Zn2-Zn3A), respectively.

Topology analysis shows the network of **4** can be rationalized to an unusual 3D trinodal (3,4,6)-connected net with $(3\cdot4\cdot5\cdot6^2\cdot7)(3\cdot4\cdot5\cdot6^7\cdot7^3\cdot8^2)(3\cdot7^2)$ topology by denoting the DDB^{4-} ligand as 3-connected nodes, the $[Zn_2(COO)_4]$ SBUs as 4-connected nodes, and the $[Zn_2(COO)_2]$ SBUs as 6-connected nodes, respectively (Fig. 4d).

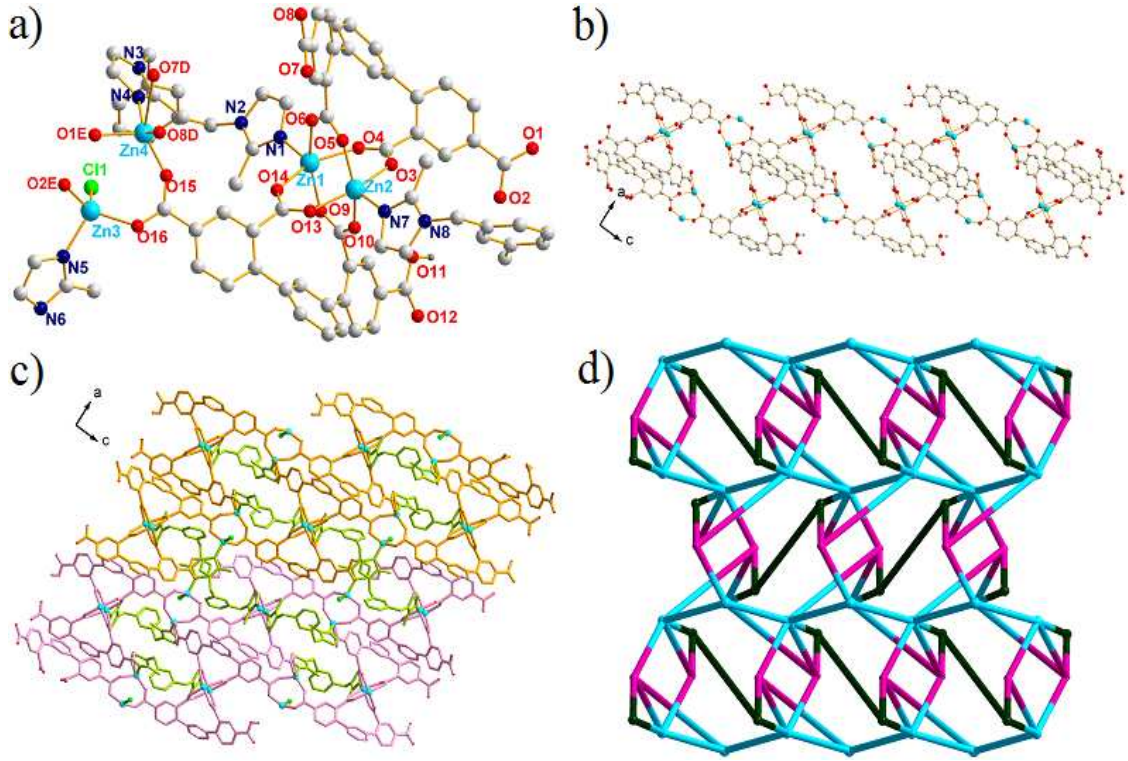

Figure 4. (a) The asymmetric unit of **4** (Symmetry codes: D: 1-*x*, 2-*y*, -*z*; E: -1/2+*x*, 3/2-*y*, -1/2+*z*.). (b) The unprecedented 2D $[Zn_2(DDB)(HDDB)]_n$ sheet view along *b* direction. (c) View of the 3D frameworks of complex **4** along *b* direction. (d) Schematic view of the novel (3,4,6)-connected net with Point Schläfli symbol of $(3\cdot4\cdot5\cdot6^2\cdot7)(3\cdot4\cdot5\cdot6^7\cdot7^3\cdot8^2)(3\cdot7^2)$.

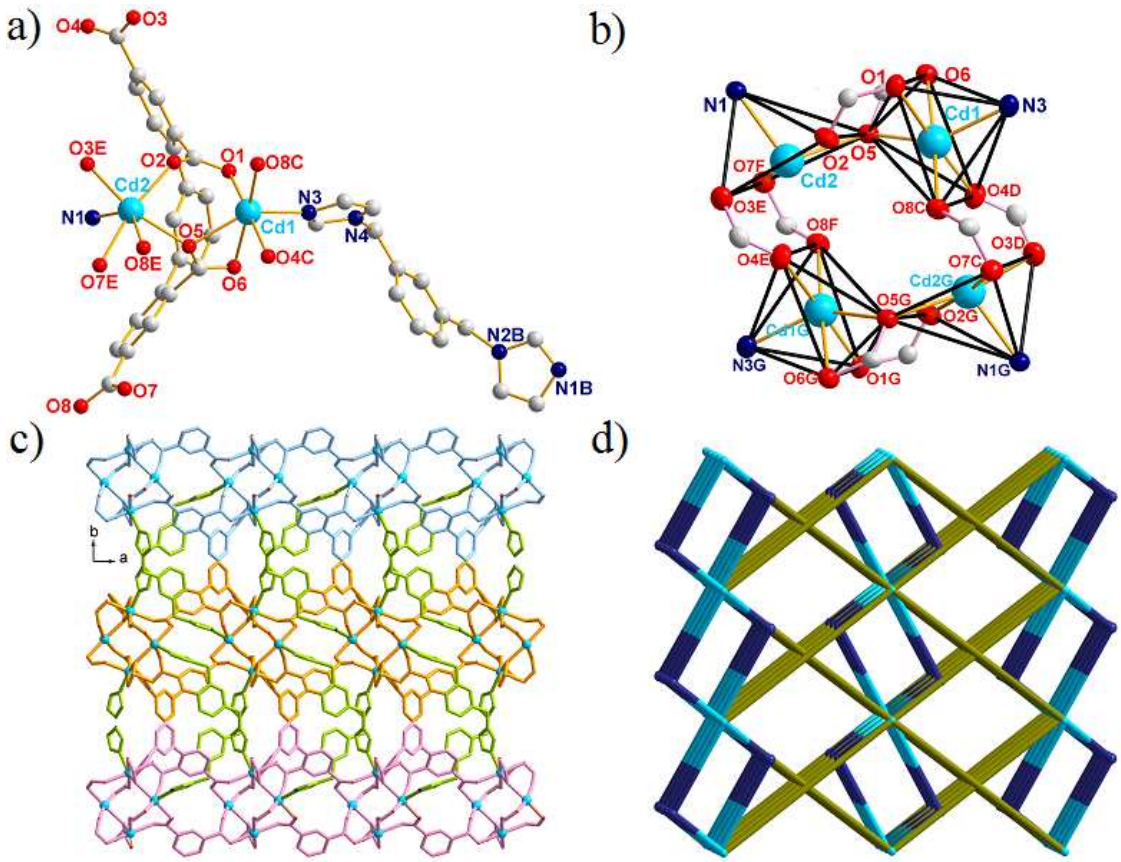

Figure 5. (a) The asymmetric unit of **5** (Symmetry codes: B: 1+*x*, 1/2-*y*, 1/2+*z*; E: -*x*, -*y*, 1-*z*; F: 1-*x*, -*y*, -*z*.). (b) The 2D $[Cd_2(DDB)]_n$ sheet in complex **5**. (c) View of the 3D frameworks of complex **5** along *c* direction. (d) The (3,10)-connected $(4^{10}\cdot6^{32}\cdot8^3)(4^3)_2$ net of complex **5**.

Structural Description of $\{[Cd_2(DDB)(1,3\text{-bimb})]\cdot H_2O\}_n$ (5). Complex **5** crystallizes in the monoclinic system $P2_1/c$ and the asymmetric unit contains two Cd^{II} ions, one DDB^{4-} ligand, two 1,3-bimb ligands, and one lattice water molecule (Fig. 5a). Cd (1) is hexa-coordinated by five O atoms from two distinct DDB^{4-} ligands and one N atom from one 1,3-bimb ligand, showing a distorted octahedral geometry. Cd(2) is located in a similar distorted octahedral environment, completed by one N atom from one 1,3-bimb ligand and five O atoms from two different DDB^{4-} ligands. The Cd−N band lengths are 2.212(13) and 2.269(12) Å, and the Cd−O distances are in the range of 2.249(10)–2.462(10) Å, respectively.

In complex **5**, H_4DDB is completely deprotonated and exhibits $(\kappa^1\text{-}\kappa^1)\text{-}(\kappa^1\text{-}\kappa^2)\text{-}(\kappa^1\text{-}\kappa^1)\text{-}(\kappa^1\text{-}\kappa^1)\text{-}\mu_6$ coordination mode (Mode V). Two Cd(1) and two Cd(2) ions are bridged by eight carboxyl groups to form an unprecedented tetranuclear $\{Cd_4(COO)_8\}$ SBUs, with the nearest Cd···Cd distances being 4.001 Å (Cd1-Cd2), and 3.949 Å (Cd1G-Cd2), respectively (Fig. 5b). The tetranuclear $\{Cd_4(COO)_8\}$ SBUs linked by the DDB^{4-} ligands to generate a 2D bilayer (Fig. S5). Those 2D $[Cd_2(DDB)]_n$ sheets are further expanded to form a 3D framework by linking the bridging 1,3-bimb ligands (Fig. 5c).

From the standpoint of topology, the final structure of **5** can be defined as a (3,10)-connected net with the Schläfli symbol of $(4^{10}\cdot6^{32}\cdot8^3)(4^3)_2$ by denoting DDB^{4-} and $\{Cd_4(COO)_8\}$ to 3–connected and 10–connected nodes, respectively (Fig. 5d).

Structural Description of $\{[Cd_2(DDB)(1,3\text{-bmib})(H_2O)_{0.5}]\cdot H_2O\}_n$ (6). With 1,3-bmib being replaced by 1,3-bimb, a similar 3D architecture was obtained, which also consisted of a similar tetranuclear $[Cd_4(COO)_8(\mu_2\text{-}H_2O)]$ SBUs. Complex **6** crystallizes in monoclinic space group $P2_1/c$. The asymmetric unit contains two crystallographically independent Cd^{II} ions, one 1,3-bmib ligand, one DDB^{4-} ligand, a half of μ_2-coordinated water molecules, and one lattice water molecule (Fig. 6a).

In complex **6**, both Cd(1) and Cd(2) ions are located in a similar distorted octahedral environment, completed by one N atom from one 1,3-bmib ligand and five O atoms from two different DDB^{4-} ligands. The Cd−N/O distances are in the range of 2.230(5)−2.577(6) Å, respectively. The DDB^{4-} anion connects the $[Cd_4(COO)_8(\mu_2\text{-}H_2O)]$ SBUs to form a 3D framework with open channels (9.495×14.984 $Å^2$) along *b* direction (Fig. 6b). And the 1,3-bmib twisted itself to fulfil the channels, finally resulting in a 3D framework (Fig. 6c). To fully comprehend this crystal structure of complex **6**, the topology analysis illustrated this 3D framework is a also a (3,10)-connected $(4^{10}\cdot6^{32}\cdot8^3)(4^3)_2$ net with the extended symbol is [4.4.4.4.4.4.4.4.4.6(2).6(2).6(2).6(2).6(2).6(2).6(2).6(2).6(4).6(4).6(4).6(4).6(4).6(4).6(4).6(4).6(4).6(4).6(4).6(4).6(4).6(4).6(4).6(4).6(4).6(4).6(4).6(4).6(4).6(4).6(4).6(4).6(4).6(4).8(8).8(20).8(44)][4.4.4][4.4.4] (Fig. 6d).

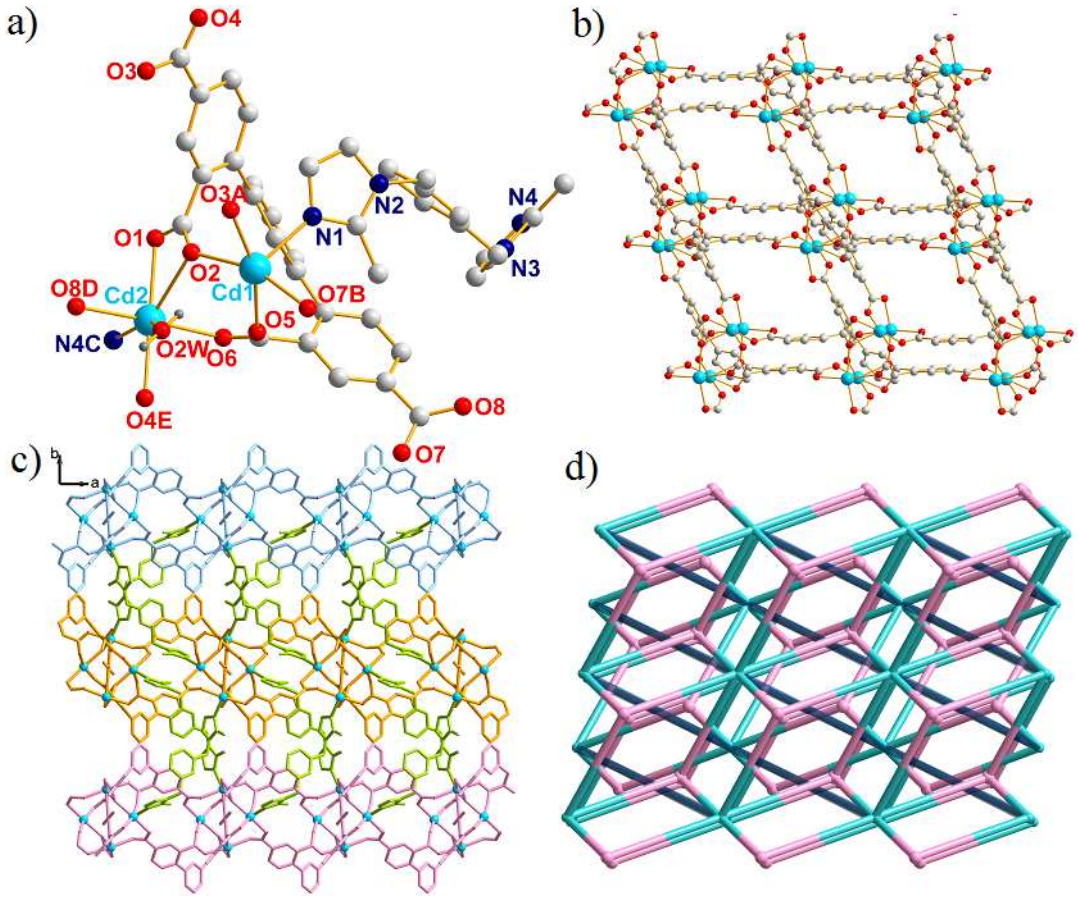

Figure 6. (a) The asymmetric unit of **6** (Symmetry codes: A: 1–*x*, –*y*, 1–*z*; B: –*x*, –*y*, 2–*z*; C: 1+*x*, 1/2–*y*, 1/2+*z*; D: 1+*x*, *y*, *z*; E: *x*, *y*, 1+*z*.). (b) The 2D $[Cd_2(DDB)]_n$ bilayer. (c) Schematic view of the 3D frameworks of **6** along *c* direction. (d) The 3D (3,6)-connected $(3\cdot6\cdot7)(3^2\cdot4^3\cdot5^4\cdot6^3\cdot7\cdot8^2)$ net of **6**.

Table 3 The detailed comparisons of complexes **1**–**6**.

Complex	Coord. Modes	Ancillary Ligands/Role	Dihedral Angles (°) of H_xDDB	Final Structure and Topology
1	Mode I	N/A	49.9(8)/31.7(1)/49.9(8)	1D chain based supramolecular
2	Mode II	1,4-bimb/bridging	47.3(1)/48.8(0)/48.2(1)	3D (3,4,6)-connected $(5^2\cdot6^2\cdot8\cdot9)(5^2\cdot6)_2(5^4\cdot6^4\cdot7^2\cdot8^3\cdot9\cdot10)$ net
3	Mode II	1,3-bimb/bridging	52.1(0)/52.1(2)/49.9(0)	3D (3,4,6)-connected $(5^2\cdot6^2\cdot8\cdot9)(5^2\cdot6)_2(5^4\cdot6^4\cdot7^2\cdot8^3\cdot9\cdot10)$ net
4	Mode III	1,3-bmib/bridging	45.3(5)/51.4(2)/46.3(6)	3D (3,4,6)-connected $(3\cdot4\cdot5\cdot6^2\cdot7)(3\cdot4\cdot5\cdot6^7\cdot7^3\cdot8^2)(3\cdot7^2)$ net
4	Mode IV	1,3-bmib/bridging	48.2(2)/37.2(6)/42.2(4)	3D (3,4,6)-connected $(3\cdot4\cdot5\cdot6^2\cdot7)(3\cdot4\cdot5\cdot6^7\cdot7^3\cdot8^2)(3\cdot7^2)$ net
5	Mode V	1,3-bimb/bridging	51.6(7)/49.0(9)/66.1(9)	3D (3,10)-connected $(4^{10}\cdot6^{32}\cdot8^3)(4^3)_2$ net
6	Mode V	1,3-bmib/bridging	51.0(0)/49.4(1)/58.8(9)	3D (3,10)-connected $(4^{10}\cdot6^{32}\cdot8^3)(4^3)_2$ net

Structural Comparsions. As shown in the Scheme 3 and Table 3, Four Zn^{II} CPs and two Cd^{II} CPs with structural diversities obtained from the solvothermal reactions of W-shaped tetracarboxylate and Zn^{II}/Cd^{II} ions, in which H_4DDB displays rich different coordination modes. In complex **1**, Two 2-position carboxyl groups were deprotonated and coordinated to one Zn^{II} ion form basic units, which are bridged by μ_2-coordinated water molecules to form 1D $[Ni(H_2O)_2(\mu_2\text{-}H_2O)]_n$ chain. Complex **2** and complex **3** are isomorphism and consists of two types of paddlewheel secondary building units (SBUs): $[Zn_2(COO)_4]$, and $[Zn_2(COO)_2]$, based on which $(5^2\cdot6^2\cdot8\cdot9)(5^2\cdot6)_2(5^4\cdot6^4\cdot7^2\cdot8^3\cdot9\cdot10)$ net is formed. In complex **4**, two independent DDB^{4-} ligands adopted $(\kappa^1\text{-}\kappa^1)\text{-}(\kappa^1\text{-}\kappa^1)\text{-}(\kappa^1\text{-}\kappa^1)\text{-}\mu_4$ and $(\kappa^1\text{-}\kappa^0)\text{-}(\kappa^1\text{-}\kappa^1)\text{-}(\kappa^1\text{-}\kappa^1)\text{-}(\kappa^1\text{-}\kappa^1)\text{-}\mu_5$ coordination modes, linking $[Zn_2(COO)_4]$ and $[Zn_2(COO)_2]$ SBUs to form a 2D $[Zn_2(DDB)(HDDB)]_n$ sheet, which are further expanded to generate a 3D (3,4,6)-connected $(3\cdot4\cdot5\cdot6^2\cdot7)(3\cdot4\cdot5\cdot6^7\cdot7^3\cdot8^2)(3\cdot7^2)$ net. For the Cd^{II} CPs, although the 1,3-bimb and 1,3-bmib ancially ligands have different rigidity, they show the same (3,10)-connected $(4^{10}\cdot6^{32}\cdot8^3)(4^3)_2$ nets, containing $[Cd_4(COO)_8]$ and $[Cd_4(COO)_8(\mu_2\text{-}H_2O)]$ SBUs, respectively. Systematic comparisons among them indicated the W-shaped H_4DDB is a good candidate to construct 3D noninterpenetrated structures due to that two adjancent 2-position carboxyl groups are inclined to form SBUs during the self-assembly process.

Thermal Analyses. The experiments of thermogravimetric analysis (TG) were performed on samples of **1**–**6**, shown in Fig.S6. For complex **1**, the TGA curve shows the weight loss of 6.9 % in the range of 60-140 °C, which corresponds to the loss of coordinated water molecules (7.1 %). And then the networks remains stable until the temperature up to 285 °C, finally the complex was pyrolyzed with a result of thermal decomposition of ZnO (Found 15.73 %, calcd. 15.51 %). For complex **2**, the whole structure began to collapse at about 340°C with a result of thermal decomposition (ZnO, obsd. 22.4%, calcd. 21.1%). For complex **3**, the whole curve is similar with **1**, the frameworks

begin to collapse at about 310°C, and final given the residual weight is ca. 22.1% (ZnO, calc. 21.1 %). For complex **4**, the first weight loss below 105 °C can be attributed to the release of lattice water (obsd: 1.3%; calcd: 1.1%). With the temperature increasing, the host network begins to collapse at about 350 °C and final given the residual weight is ca. 19.8% (ZnO, calc. 19.7%). For **5**, the weight loss of water molecules is observed at about 95 °C (obsd: 2.6 % and calcd: 2.0 %). The decomposition of organic ligands began from 350 °C, with a result of thermal decomposition (obsd. 29.6%, calcd. 29.1%). For complex **6**, the release of lattice and coordinated water molecules (obsd: 3.0%; calcd: 2.9%) took place in the temperature range of 85–135 °C and the framework is stable below 350°C. Above this temperature, the networks collapsed and finally given a thermal decomposition.

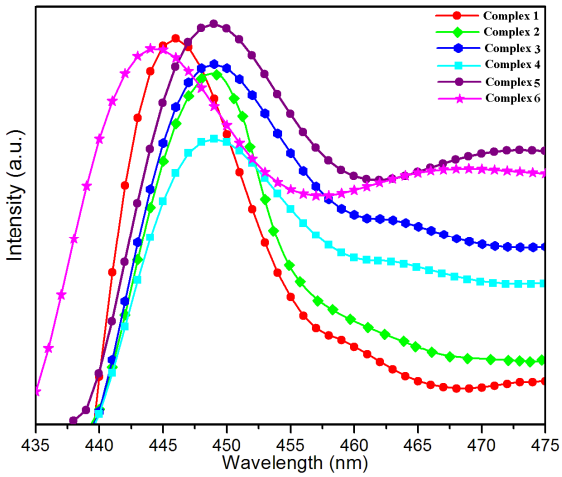

Figure 7. Emission spectra of complexes **1-6** in the solid state at room temperature.

Photoluminescence Properties. Many d^{10} transition metal coordination polymers have been extensively studied due to their potential applications as luminescent materials.[17] The solid state luminescent properties of complexes **1-6** and the free H_4DDB ligand were investigated at room temperature.

As shown in Fig. S7, the free H_4DDB ligand show violet fluorescent emission band at 403 nm under 373 nm wavelength excitation, which can be mainly attributed to the π*→n or π*→π transitions.[18] For complexes **1-6**, the emission spectra exhibit strong blue-fluorescent emission peaks at 446 nm (λ_{ex} = 423 nm) for **1**, 449 nm (λ_{ex} = 427 nm) for **2**, 448 nm (λ_{ex} = 427 nm) for **3**, 445 nm (λ_{ex} = 423 nm) for **4**, 451 nm (λ_{ex} = 427 nm) for **5**, and 446 nm (λ_{ex} = 423 nm) for **6**, respectively, which could be assigned to the intraligand emission (π*→n or π*→π) because these emissions are neither metal-to-ligand charge transfer (MLCT) nor ligand-to-metal transfer (LMCT) in nature since the d^{10} Zn^{II}/Cd^{II} ions are difficult to oxidize or reduce.[19] The difference of the emission behaviours of those complexes probably derives from the different conformations of organic ligands and the differences in the rigidity of solid state crystal packing structures.[20]

Photocatalytic Properties. Complexes **1-6** display strong blue fluorescence in the solid state at room temperature, indicating they are good candidates for photoactive materials. To investigate the photocatalytic activity of complexes **1-6**, methylene orange (MO) was selected as a model dye contaminant to evaluate the photocatalytic activities for the purification of waste water. As illustrated in Fig. 8 and Fig. 9, the variations of the Mo concentration were plotted versus irradiation time. The total catalytic degradation efficiency of the controlled experiment is 5.9 % after 60 min (Fig. S8). The plots show that the degradation efficiency of MO after 60 min is 17.6 % for complex **1**, 63.2 % for **2**, 78.4 % for **3**, 75.3 % for **4**, 99.8 % for **5**, and 99.5 % for **6**, respectively. The absorption peaks of MO decreased obviously under the UV in the presence of **5** and **6**, slowly in the presence of **2**, **3** and **4**, and very slowly in the presence of **1**. The reason may be derived from the difference of components and structures.[21] The central metal ions as well as the organic linkers are involved in the photocatalytic process.

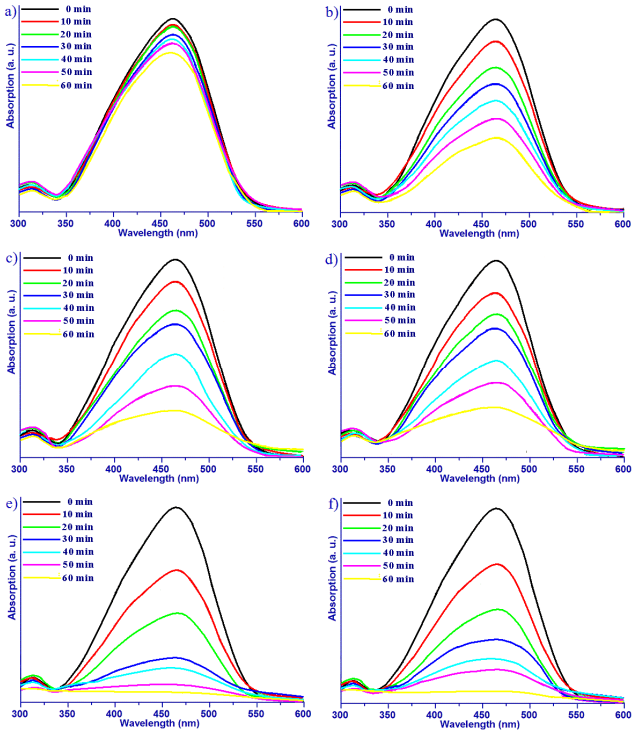

Figure 8. UV-Vis absorption spectra of the MO solutions degraded by different photocatalysts under UV irradiation at different time intervals: (a) **1** in MO; (b) **2** in MO; (c) **3** in MO; (d) **4** in MO; (e) **5** in MO; and (f) **6** in MO.

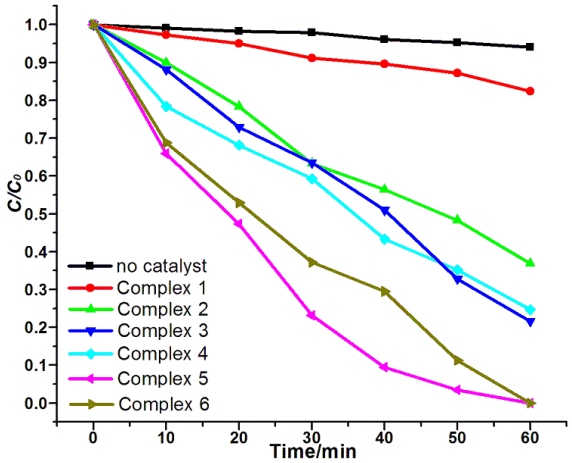

Figure 9. Photocatalytic decomposition of MO in aqueous solution under UV light irradiation with the use of complexes **1**–**6** and the control experiment without any catalyst.

The possible mechanism for the MO degradation is proposed as described in the previous literature.[22] Under the irradiation of UV-Vis light, the bis(imidazole) linkers and DDB anions are induced to produce O or N-metal charge transfer and promote electron transformations from the highest occupied molecular orbital (HOMO) to the lowest unoccupied molecular orbital (LUMO). Therefore, the HOMO strongly needs one electron to return to its stable state. Thus, one electron was captured from water molecules, which was oxygenated to generate the ·OH radicals. And then the ·OH active species could decompose the MO effectively to complete the photocatalytic process. The colour and the PXRD of the recovered samples from photocatalytic experiments showed no changement. The result indicates that the catalyst may be recycled from the catalytic experiments.

Conclusions

In summary, successful synthesis of six d^{10} CPs proved that the W-shaped teretetracarboxylate ligand is a good candidate for constructing high-connected architectures due to that di- or tetra-dinuclear SUBs could be easily formed with the linkage of two 2-position carboxylate groups. Complexes **2**-**6** displayed 3D noninterpenetrated framework with appealing structural features varying from 3D (3,4,6)-connected $(5^2\cdot6^2\cdot8\cdot9)(5^2\cdot6)_2(5^4\cdot6^4\cdot7^2\cdot8^3\cdot9\cdot10)$ net for **2** and **3**, (3,4,6)-connected $(3\cdot4\cdot5\cdot6^2\cdot7)(3\cdot4\cdot5\cdot6^7\cdot7^3\cdot8^2)(3\cdot7^2)$ for **4**, to 3D (3,10)-connected $(4^{10}\cdot6^{32}\cdot8^3)(4^3)_2$ net for **5** and **6**, which have never been documented to date. Moreover, complexes **1**-**6** are excellent blue-fluorescent luminescent materials, which show relatively good photocatalytic activity for dye methylene orange (MO) degradation in aqueous solution under UV light.

Acknowledgements

The work was supported by financial support from the Natural Science Foundation of China (Grant Nos. 21101097, 21451001), key discipline and innovation team of Qilu Normal University.

Notes

The authors declare no competing financial interest.

References

1. (a) G. Férey and C. Serre, *Chem. Soc. Rev*., 2009, **38**, 1380; (b) Z. H. Wang, D. F. Wang, T. Zhang, R. B. Huang and L. S. Zheng, *CrystEngComm*, 2014, **16**, 5028; (c) W. Shi, S. Song and H. Zhang, *Chem. Soc. Rev*., 2013, **42**, 5714; (d) K. Wang, S. Zeng, H. Wang, J. Dou and J. Jiang, *Inong. Chem. Front.*, 2014, **1**, 167; (e) W. L. Leong and J. J. Vittal, *Chem. Rev.*, 2011, **111**, 688; (f) A. Mallick, B. Garai, M.A. Addicoat, P.S. Petkov, T. Heine and R. Banerjee, *Chem. Sci.*, 2015, **6**, 1420.
2. (a) D. Balaji Shinde, S. Kandambeth, P. Pachfule, R. R.Kumar and R.Banerjee, *Chem. Commun.*, 2015, **51**, 310; (b) J. Duan, M. Higuchi, R. Krishna, T. Kiyonaga, Y. Tsutsumi, Y. Sato, Y. Kubota, M. Takata and S. Kitagawa, *Chem. Sci.*, 2014, **5**, 660; (c) P. V. Dau and S. M. Cohen, *Chem. Commun.*, 2013, **49**, 6128; (d) J. P. Zhang, P. Q. Liao, H. L. Zhou, R. B. Lin and X. M. Chen, *Chem. Soc. Rev*., 2014, **43**, 5789; (e) L. Fan, W. Fan, W. Song, G. Liu, X. Zhang and X. Zhao, *CrystEngComm*, 2014, **16**, 9191; (f) D. S. Li, Y. P. Wu, J. Zhao, J. Zhang and J. Y. Lu, *Coord. Chem. Rev*., 2014, **261**, 1.
3. (a) U. P. Singh, S. Narang, P. Pachfule and R. Banerjee, *CrystEngComm*, 2014, **16**, 5012; (b) E. D. Bloch, W. L. Queen, R. Krishna, J. M. Zadrozny, C. M. Brown and J. R. Long, *Science*, 2012, **335**, 1606; (c) S. Chen, R. Shang, K. L. Hu, Z. M. Wang and S. Gao, *Inong. Chem. Front*., 2014, **1**, 83; (d) X. T. Zhang, D. Sun, B. Li, L. M. Fan, B. Li and P. H. Wei, *Cryst. Growth Des.*, 2012, **12**, 3845; (e) S. L. Huang, Y. J. Lin, T. S. A. Hor and G. X. Jin, *J. Am. Chem. Soc*., 2013, **135**, 8125.
4. (a) T. Panda, K. M. Gupta, J. Jiang and R. Banerjee, *CrystEngComm*, 2014, **16**, 4677; (b) T. Wu, Y. J. Lin and G. X. Jin, *Dalton Trans.*, 2014, **43**, 2356; (c) X. T. Zhang, L. M. Fan, X. Zhao, D. Sun, D. C. Li and J. M. Dou, *CrystEngComm*, 2012, **14**, 2053; (d) J. B. Lin, W. Xue, B. Y. Wang, J. Tao, W. X. Zhang, J. P. Zhang and X. M. Chen, *Inorg. Chem*., 2012, **51**, 9423; (e) X. Zhang, L. Fan, W. Zhang, Y. Ding, W. Fan and X. Zhao, *Dalton Trans.,* 2013, **42**, 16562; (f) H. Li, Y. F. Han, Y. J. Lin, Z. W. Guo and G. X. Jin, *J. Am. Chem. Soc*., 2014, **136**, 2982; (g) X. Zhang, L. Fan, Z. Sun, W. Zhang, W. Fan, L. Sun and X. Zhao, *CrystEngComm*, 2013, **15**, 4910.
5. (a) J. Z. Qiao, M. S. Zhan and T. P. Hu, *RSC Adv.*, 2014, **4**, 62285; (b) C. Zhan, C. Zou, G. Q. Kong and C. D. Wu, *Cryst. Growth Des.*, 2013, **13**, 1429; (c) X. Chang, Y. Zhao, M. Han, L. Ma and L. Wang, *CrystEngComm*, 2014, **16**, 6417; (d) D. S. Li, X. J. Ke, J. Zhao, M. Du, K. Zou, Q. F. He and C. Li, *CrystEngComm*, 2011, **13**, 3355.
6. (a) U. J. Williams, B. D. Mahoney, A. J. Lewis, P. T. DeGregorio, P. J. Carroll and E. J. Schelter, *Inorg. Chem.*, 2013, **52**, 4142; (b) Y. W. Li, D. C. Li, J. Xu, H. G. Hao, S. N. Wang, J. M. Dou, T. L. Hu and X. H. Bu, *Dalton Trans.,* 2014, **43**, 15708; (c) Q. Zhang, H. Zhang, S. Zeng, D. Sun and C. Zhang, *Chem-Asian J.*, 2013, **8**, 1985; (d) S. Q. Zhang, F. L. Jiang, M. Y. Wu, L. Chen, J. H. Luo and M. C. Hong, *CrystEngComm*, 2013, **15**, 3992.
7. (a) X. H. Chang, J. H. Qin, M. L. Han, L. F. Ma and L. Y. Han, *CrystEngComm*, 2014, **16**, 870; (b) N. Zhang, Y. Tai, M. Liu, P. Ma, J. Zhao and J. Niu, *Dalton Trans.,* 2014, **43**, 5182; (c) W. Meng, Z. Xu, J. Ding, D. Wu, X. Han, H. Hou and Y. Fan, *Cryst. Growth Des.*, 2014, **14**, 730; (d) L. Liu, C. Yu, J. Sun, P. Meng, F. Ma, J. Du and L. Ma, *Dalton Trans.,* 2014, **43**, 2915.
8. (a) F. Guo, B. Zhu, M. Liu, X. Zhang, J. Zhang and J. Zhao, *CrystEngComm*, 2013, **15**, 6191; (b) Y. B. Wang, Y. L. Lei, S. H. Chi and Y. J. Luo, *Dalton Trans.,* 2013, **42**, 1862; (c) X. Zhang, L. Fan, W. Zhang, W. Fan, L. Sun and X. Zhao, *CrystEngComm*, 2014, **16**, 3203; (d) X. Chang, J. Qin, M. Han, L. Ma and L. Wang, *CrystEngComm*, 2014, **16**, 870.
9. (a) L. Fan, W. Fan, B. Li, X. Liu, X. Zhao and X. Zhang, *Dalton Trans.,* 2015, **44**, 2380; (b) C. Zhan, C. Zou, G. Q. Kong and C. D. Wu, *Cryst. Growth Des*., 2013, **13**, 1429; (c) L. Fan, Y. Gao, G. Liu, W. Fan, W. Song, L. Sun, X. Zhao and X. Zhang, *CrystEngComm*, 2014, **16**, 7649; (d) M. Meng, D. C. Zhong and T. B. Lu, *CrystEngComm*, 2011, **13**, 6794.
10. (a) L. Fan, W. Fan, B. Li, X. Zhao and X. Zhang, *RSC Adv.*, 2015, **5**, 39854; (b) B. Guo, L. Li, Y. Wang, Y. Zhu and G. Li, *CrystEngComm*, 2013, **42**, 14268; (c) L. Fan, X. Zhang, W. Zhang, Y. Ding, W. Fan, L. Sun, Y. Pang and X. Zhao, *Dalton Trans.,* 2014, **43**, 6701; (d) L. Fan, W. Fan, B. Li, X. Liu, X. Zhao and X. Zhang, *CrystEngComm*, 2015, **17**, 4669.
11. (a) Y. F. He, D. M. Chen, H. Xu and P. Chen, *CrystEngComm*, 2015, **17**, 2471; (b) Q. Yang, L. Huang, M. Zhang, Y. Li, H. Zheng and Q. Lu, *Cryst. Growth Des*., 2013, **13**, 440; (c) H. L. Jiang, B. Liu and Q. Xu, *Cryst. Growth Des*., 2010, **10**, 806; (d) S. N. Zhao, S. Q. Su, X. Z. Song, M. Zhu, Z. M. Hao, X. Meng, S. Y. Song and H. J. Zhang, *Cryst. Growth Des*., 2013, **13**, 2756.
12. (a) Y. Y. Yang, Z. J. Lin, T. T. Liu, J. Liang and R. Cao, *CrystEngComm*, 2015, **17**, 1381; (b)Y. H. Tan, J. B. Xiong, J. X. Gao, Q. Xu, C. W. Fu, Y. Z. Tang, S. P. Yang, H. R. Wen and Q. Shu, *RSC Adv.*, 2015, **5**, 30216; (c) L. L. Liu, C. X. Yu, F. J. Ma, Y. R. Li, J. J. Han, L, Lin and L. F. Ma, *Dalton Trans.,* 2015, **44**, 1636.
13. (a) S. Q. Zang, F. L. Jiang, M. Y. Wu, J. Ma, Y. Bu and M. C. Hong, *Cryst. Growth Des*., 2012, **12**, 1452; (b) H. Zhou, G. X. Liu, X. F.

Wang and Y. Wang, *CrystEngComm*, 2013, **15**, 1377; (c) Q. Yang, X. Chen, J. Cui, J. Hu, M. Zhang, L. Qin, G. Wang, Q. Lu and H. Zheng, *Cryst. Growth Des*., 2012, **12**, 4072; (d) Q. Yang, X. Chen, Z. Chen, Y. Hao, Y. Li, Q. Lu and H. Zheng, *Chem. Commun.,* 2012, **48**, 10016.

14. (a) T. Wu, Y. J. Lin and G. X. Jin, *Dalton Trans.*, 2014, **42**, 82; (b) L. Fan, X. Zhang, Z. Sun, W. Zhang, Y. Ding, W. Fan, L. Sun, X. Zhao and H. Lei, *Cryst. Growth Des.*, 2013, **13**, 2462; (c) X. T. Zhang, L. M. Fan, Z. Sun, W. Zhang, D. C. Li, J. M. Dou and L. Han, *Cryst. Growth Des*., 2013, **13**, 792; (d) L. Fan, W. Fan, W. Song, L. Sun, X. Zhao and X. Zhang, *Dalton Trans.,* 2014, **43**, 15979; (e) L. Fan, X. Zhang, W. Zhang, Y. Ding, W. Fan, L. Sun and X. Zhao, *CrystEngComm*, 2014, **16**, 2144.
15. (a) G. M. Sheldrick, *SHELXTL*, version 5.1; Bruker Analytical X-ray Instruments Inc.: Madison, WI, 1998. (b) G. M. Sheldrick, *SHELX-97*, PC Version; University of Gottingen: Gottingen, Germany, 1997.
16. (a) V. A. Blatov, A. P. Shevchenko and V. N. Serezhkin, *J. Appl. Crystallogr.*, 2000, **33**, 1193; (b) The network topology was evaluated by the program "TOPOS-4.0", see: http://www.topos.ssu.samara.ru. (c) V. A. Blatov, M. O'Keeffe and D. M. Proserpio, *CrystEngComm*, 2010, **12**, 44.
17. (a) Y. L. Cai, F. L. Jiang, L. Chen, Y. Bu, M. Y. Wu, K. Zhou, J. Pang and M. C. Hong, *Dalton Trans.,* 2013, **42**, 9954; (b) L. L. Han, T. P. Hu, K. Mei, Z. M. Guo, C. Yin, Y. X. Wang, J. Zheng, X. P. Wang and D. Sun, *Dalton Trans.,* 2015, **44**, 6052; (c) L. L. Liu, C. X. Yu, Y. R. Li, J. J. Han, F. J. Ma and L. F. Ma, *CrystEngComm*, 2015, **17**,653.
18. (a) X. Y. Wang, F. L. Jiang, L. Chen, J. Pan, K. Zhou, K. Z. Su, J. D. Pang, G. X. Lyu and M. C. Hong, *CrystEngComm*, 2015, **17**, 3829; (b) S. Yuan, Y. K. Deng, W. M. Xuan, X. P. Wang, S. N. Wang, J. M. Dou and D. Sun, *CrystEngComm*, 2014, **16**, 3829; (c) T. Liu, S. Wang, J. Lu, J. Dou, M. Niu, D. Li and J. Bai, *CrystEngComm*, 2013, **15**, 5476.
19. (a) T. Cao, Y. Peng, T. Liu, S. Wang, J. Dou, Y. Li, C. Zhou, D. Li and J. Bai, *CrystEngComm*, 2014, **16**, 10658; (b) Z. H. Yan, L. L. Han, Y. Q. Zhao, X. Y. Li, X. P. Wang, L. Wang and D. Sun, *CrystEngComm*, 2014, **16**, 8747; (c) L. Fan, W. Fan, B. Li, X. Liu, X. Zhao and X. Zhang, *RSC Adv.*, 2015, **5**, 14897.
20. (a) J. Pan, F. L. Jiang, M. Y. Wu, L. Chen, J. J. Qian, K. Z. Su, X. Y. Wan and M. C. Hong, *CrystEngComm*, 2014, **16**, 11078; (b) X. Zhang, L. Fan, W. Song, W. Fan, L. Sun and X. Zhao, *RSC Adv.*, 2014, **5**, 30274; (c) L. Fan, X. Zhang, D. Li, D. Sun, W. Zhang and J. Dou, *CrystEngComm*, 2013, **15**, 349.
21. (a) X. Wang, J. Huang, L. Liu, G. Liu, H. Lin, J. Zhang, N. Chen and Y. Qu, *CrystEngComm*, 2013, **15**, 1960; (b) P. Du, Y. Yang, J. Yang, B. K. Liu and J. F. Ma, *Dalton Trans.*, 2013, **42**, 1567; (c) D. X. Li, C. Y. Ni, M. M. Chen, M. Dai, W. H. Zhang, W. Y. Yan, H. X. Qi, Z. G. Ren and J. P. Lang, *CrystEngComm*, 2014, **16**, 2158; (d) L. Zhou, C. Wang, X. Zheng, Z. Tian, L. Wen, H. Qu and D. Li, *Dalton Trans.*, 2013, **42**, 16375; (e) M. Li, L. Liu, L. Zhang, X. Lv, J. Ding, H. Hou and Y. Fan, *CrystEngComm*, 2014, **16**, 6408.
22. (a) J. Hao, B. Yu, K. V. Hecke and G. Cui, *CrystEngComm*, 2015, **17**, 2279; (b) Y. F. Peng, S. Zhao, K. Li, L. Liu, B. L. Li and B. Wu, *CrystEngComm*, 2015, **17**, 2544; (c) L. Liu, J. Ding, M. Li, Xi. Lv, J. Wu, H. Hou and Y. Fan, *Dalton Trans.*, 2014, **43**, 12790; (d) W. Y. Yin, Z. L. Huang, X. Y. Tang, J. Wang, H. J. Cheng, Y. S. Ma, R. X. Yuan and D. Liu, *New J. Chem.*, 2015, DOI: 10.1039/C5NJ01005E.

CrystEngComm

For Table of Contents Use Only

Table of Contents Graphic and Synopsis

Assembly of A Series of d^{10} Coordination Polymers Based on W-shaped 1,3-Di(2',4'-dicarboxylphenyl)benzene: From Syntheses, Structural Diversity, Luminescence, to Photocatalytic Properties

Xiutang Zhang, Liming Fan, Weiliu Fan, Bin Li and Xian Zhao

Six d^{10} coordination polymers with different architectures based on W-shaped 1,3-di(2',4'-dicarboxylphenyl)benzene (H_4DDB) have been prepared. Their photoluminescence and photocatalytic properties were also investigated.